

1 **Influence of axial length on ganglion cell complex (GCC) thickness and on GCC**
2 **thickness to retinal thickness ratios in young adults.**

3 Asuka Takeyama, Yoshiyuki Kita, Ritsuko Kita, Goji Tomita

4 Department of Ophthalmology, Toho University Ohashi Medical Center, Tokyo, Japan

5
6 **Running title:** Influence of axial length on *G/T* ratio

7
8 **Corresponding author:** Yoshiyuki Kita, Department of Ophthalmology, Toho University Ohashi
9 Medical Center, 2-17-6 Ohashi, Meguro-ku, Tokyo 153-8515, Japan

10 Fax number: +81-3-3468-2926

11 Telephone number: +81-3-3468-1251

12 E-mail address: kitakita220@gmail.com

13
14
15
16 **Declaration of competing/conflicts of interest:**

17 The authors declare no conflict of interest.

18 **Declaration of funding sources:**

19 This study was supported in part by a Grant-in-Aid for Scientific Research (C) 24592656 from the
20 Ministry of Education, Culture, Sports, and Technology of the Japanese Government.

21
22
23
24
25
26
27
28

29 **Abstract**

30 *Purpose*

31 The present study was designed to investigate the influence of axial length on macular ganglion cell
32 complex (GCC) thickness and two ratio parameters—the GCC thickness to macular total retinal
33 thickness (*G/T*) ratio and the GCC thickness to macular outer retinal thickness (*G/O*) ratio—using
34 spectral-domain optical coherence tomography (OCT)

35 *Methods*

36 In this prospective case series, 74 eyes of 74 healthy Japanese study participants with varying degrees
37 of myopia were recruited. GCC, outer retinal, and total retinal thicknesses were measured with the
38 RTVue-100 system. The *G/T* and *G/O* ratios were also calculated. The axial length was determined
39 using the IOLMaster. The correlation between the OCT measurements and axial length was evaluated.

40 *Results*

41 The average axial length was 25.05 ± 1.38 mm. The GCC thickness was significantly correlated with
42 axial length ($r = -0.384$, $P = 0.001$). The outer retinal thickness and the total retinal thickness were
43 significantly correlated with axial length ($r = -0.444$, $P < 0.001$ and $r = -0.493$, $P < 0.001$,
44 respectively), but the *G/T* and *G/O* ratios were not ($r = -0.093$, $P = 0.428$ and $r = -0.091$, $P = 0.440$,
45 respectively).

46 *Conclusions*

47 GCC thickness is affected by axial length. Because the prevalence of myopia is high in Japan, when
48 determining the GCC thickness of Japanese individuals, it seems necessary to consider the axial length
49 as well. To take account of individual variation in axial length, we propose the ratio parameters as a
50 suitable parameter.

51 **Keywords:** Axial length, Ganglion cell complex, Optical coherence tomography, Ratio, Refractive
52 error

53

54

55 **Introduction**

56 The prevalence of myopia is high in East Asian countries [1, 2]. An association between myopia and
57 glaucoma has been recognized, and the prevalence of myopia is increased in patients with ocular
58 hypertension, primary open-angle glaucoma, and normal-tension glaucoma [2]. However, the
59 appearance of the optic disc in myopic patients is often difficult to interpret and may mask early
60 glaucomatous damage. The visual field test also has limitations when used to detect glaucoma: it is
61 less sensitive for early glaucoma, and abnormal results frequently occur in patients with severe myopia
62 due to myopic macular degeneration. Optical coherence tomography (OCT) studies have shown that
63 decreases in the circumpapillary (cp) retinal nerve fiber layer (RNFL) thickness start from the early
64 stages of glaucoma [3–5]. Measurement of cpRNFL thickness has emerged as an important diagnostic
65 technology for glaucoma [6–9]. However, with increasing myopia, the superotemporal and
66 inferotemporal RNFL thickness bundles tend to converge temporally, thereby reducing the angle
67 bounded by the bundles. The cpRNFL thickness is not useful in highly myopic eyes because the area
68 coded as “abnormal” in the cpRNFL thickness deviation map indicates not only a decrease in cpRNFL
69 thickness in eyes with glaucoma but also the RNFL distribution in highly myopic eyes [10].

70 The diagnostic potential of the macular ganglion cell complex (GCC) thickness in the highly myopic
71 eye has been reported to be higher than that of the cpRNFL thickness [11, 12]. However, those
72 previous studies carried out with spectral domain OCT (SD-OCT) revealed that axial length influences
73 not only the cpRNFL thickness but also the GCC thickness [13–21]. Recently, we reported that new
74 macular parameters— the GCC thickness to total retinal thickness (G/T) ratio and the GCC thickness
75 to outer retinal thickness (G/O) ratio— are useful for diagnosing glaucoma with myopia [22, 23].

76 The G/T ratio represents the relative amount of the GCC thickness included in the total retinal
77 thickness. In the present study, we evaluated the influence of axial length on GCC, cpRNFL
78 measurements, and these ratio parameters.

79

80 **Study participants and methods**

81 This was a prospective case series. Healthy Japanese study participants with myopia were recruited
82 through an advertisement from September 2012 to January 2013. All participants were examined in

83 the Department of Ophthalmology, Toho University Ohashi Medical Center, Tokyo, Japan. The Toho
84 University Ohashi Medical Center Institutional Review Board approved all protocols, and the study
85 adhered to the tenets of the Declaration of Helsinki. The study protocols were thoroughly explained to
86 all participants, and written informed consent was obtained from each participant.

87 All participants underwent complete ophthalmologic examinations and assessments of their medical
88 and family histories. Ophthalmologic procedures performed included visual acuity testing with
89 refraction, slit-lamp biomicroscopy, Goldmann applanation tonometry, and dilated stereoscopic fundus
90 examination. Visual field sensitivity was determined using Humphrey field analyzer (Humphrey-Zeiss
91 Systems, Dublin, CA, USA) 24-2 Swedish interactive threshold algorithm standard automated
92 perimetry. Axial length was measured using partial laser interferometry performed with the IOLMaster
93 (Carl Zeiss Meditec, Jena, Germany). Noncycloplegic refraction was measured with an auto
94 ref-keratometer (ARK-530A; Nidek, Aichi, Japan). The refraction data were converted to the spherical
95 equivalent, which was calculated using the spherical diopter (D) plus one-half of the cylindrical
96 dioptric power.

97 Normal participants were healthy individuals who had an intraocular pressure (IOP) of <21 mmHg, a
98 normal optic nerve head (ONH) appearance without glaucomatous damage (i.e., no disc hemorrhage,
99 notching, thinning of the neural rim, or visible RNFL defect), normal open anterior chamber angles,
100 normal visual field testing results for the Glaucoma Hemifield Test (GHT), and a best-corrected visual
101 acuity of at least 1.0, with a spherical refractive error of between +3.00 and -12.0 D and a cylinder
102 correction within 3.0 D. Exclusion criteria were an IOP of ≥ 22 mmHg, evidence of a reproducible
103 visual field defect with abnormal or borderline results in the GHT, an unreliable visual field test
104 (>15 % false positives or false negatives or >20 % fixation losses), intraocular surgery, history of
105 ocular trauma, diabetes mellitus or neurologic diseases, vitreoretinal disease, evidence of macular
106 abnormality, myopic tilted disc, myopic disc with saucer-like cupping, and evidence of optic nerve or
107 RNFL abnormality.

108

109 OCT measurements

110 OCT was performed with the RTVue-100 (software version 4.0.5.39; Optovue, Fremont, CA, USA).

111 After achieving pupil dilation by instillation of 1 % tropicamide and 2.5 % phenylephrine
112 hydrochloride to the eye over a 20-min period, a well-trained operator obtained good-quality OCT
113 images. Images were excluded when the signal strength indicator was <45 owing to media opacity,
114 patient positioning, or excessive eye movement.

115 The RTVue-100 system uses a scanning laser diode to emit a scan beam of 840 ± 10 nm and provides
116 images of ocular microstructures. In this study, the GCC scanning protocol was used to determine the
117 macular total retinal thickness [measured from the inner limiting membrane (ILM) to the outer retinal
118 pigment epithelium (RPE)], GCC thickness [measured from the ILM to the outer inner plexiform
119 layers (IPL)], and outer retinal thickness (measured from the outer IPL to the outer RPE; Fig. 1). The
120 GCC protocol consists of 15 vertical line scans that cover a 7×7 -mm region. To achieve the best
121 coverage possible within the temporal region, the GCC protocol centered the scan at 1 mm temporal to
122 the center of the fovea. During the total scanning period, the GCC protocol captured 15,000 data
123 points within 0.6 s. Three types of data (average, superior, and inferior thicknesses) were used to
124 analyze the GCC, outer retinal, and total retinal thicknesses.

125 The ONH scanning protocol was used to measure the cpRNFL thickness. The total acquisition time
126 for a single scan was 0.55 s. Using the fundus picture generated by the OCT, we were able to manually
127 trace the contour of the ONH. Using the existing software, the RNFL thickness was automatically
128 measured at a diameter of 3.45 mm around the center of the optic disc. A total of 775 A scans were
129 obtained at this circumference. The cpRNFL thickness parameter was designed to evaluate the mean
130 thickness of a 360° area that includes the superior and inferior hemispheres and the temporal, superior,
131 nasal, and inferior quadrants. Cases with parapapillary atrophy that extended beyond the OCT RNFL
132 scan measurement circle were excluded. No corrections for magnification were made in any of the
133 cases.

134

135 *G/T* ratio and *G/O* ratio

136 We created two new macular parameters: the *G/T* ratio and the *G/O* ratio. These ratio parameters were
137 calculated using the following published formulae [22, 23]: *G/T* ratio (%) = (GCC thickness/macular
138 total retinal thickness) \times 100, and *G/O* ratio (%) = (GCC thickness/macular outer retinal thickness) \times

139 100.

140

141 Statistical analysis

142 Pearson's correlation coefficients and partial correlation analysis were calculated to evaluate the

143 relationships between the SD-OCT measurements and the demographic and clinical variables.

144 Multiple regression analysis was used to evaluate the relationship between the GCC and age, sex, axial

145 length, and outer retinal thickness. Statistical analysis was performed using IBM SPSS Statistics for

146 Windows (version 19.0; SPSS, Chicago, IL, USA). Probability values of <0.05 were considered

147 significant.

148

149 **Results**

150 Seventy-eight study participants were initially enrolled in the study. We excluded 4 participants

151 because of poor image analysis quality. We assessed eyes of Japanese individuals. We included 74

152 normal participants in the final analysis (47 men and 27 women; age range 22–51 years; mean age

153 34.88 ± 7.02 years). The mean axial length and spherical equivalent were 25.05 ± 1.38 mm

154 (22.25 – 28.76 mm) and -3.47 ± 2.96 D ($+1.00$ to -11.00 D), respectively. As expected, axial length and

155 refractive error were significantly correlated ($r = -0.806$, $P < 0.0001$). The participants' characteristics

156 are presented in Table 1.

157 Table 2 shows the OCT parameter measurements obtained using the RTVue-100. The average GCC

158 thickness was 93.07 ± 5.84 μ m. The average *G/T* ratio and average *G/O* ratio were 35.64 ± 1.34 and

159 55.43 ± 3.30 %, respectively.

160 Table 3 shows the relationships between the OCT parameters and the demographic and clinical

161 variables. The average cpRNFL thickness was significantly correlated with both the axial length ($r =$

162 -0.512 , $P < 0.001$) and the spherical equivalent ($r = 0.514$, $P < 0.001$). The average GCC thickness

163 was not correlated with age ($r = 0.028$, $P = 0.810$). The average GCC thickness was correlated with

164 both axial length ($r = -0.384$, $P = 0.001$) and spherical equivalent ($r = 0.436$, $P < 0.001$; Fig. 2). A

165 1-mm increase in axial length resulted in a decrease in the average GCC thickness of approximately

166 1.62 μ m. The average outer retinal thickness was correlated with both the axial length ($r = -0.444$, $P <$

167 0.001) and the spherical equivalent ($r = 0.406$, $P < 0.001$; Fig. 2).

168 Table 4 shows the relationships between the ratio parameters and the demographic and clinical
169 variables. The average G/T ratio and the average G/O ratio were not correlated with age ($r = 0.013$, P
170 $= 0.914$ and $r = 0.014$, $P = 0.904$, respectively). The average G/T ratio and G/O ratio were not
171 significantly correlated with either the axial length ($r = -0.093$, $P = 0.428$ and $r = -0.091$, $P = 0.440$,
172 respectively) or the spherical equivalent ($r = 0.173$, $P = 0.140$ and $r = 0.172$, $P = 0.144$, respectively;
173 Fig. 2).

174 Table 5 shows the results of the multiple linear regression analysis of the effects of age, sex, axial
175 length, and macular outer retinal thickness on the GCC thickness. Significant positive relationships
176 between the GCC thickness and the axial length and between the GCC thickness and the outer retinal
177 thickness were found ($P = 0.03$ and $P = 0.02$, respectively). No significant relationship was found
178 between the GCC thickness and either age or sex.

179 Partial correlation analysis was conducted. A significant correlation was found between the average
180 GCC thickness and the average outer retinal thickness (partial correlation analysis adjusted by axial
181 length: $r = 0.312$, $P = 0.007$). Also, a significant correlation was found between the average GCC
182 thickness and the axial length (partial correlation analysis adjusted by the outer retinal thickness: $r =$
183 -0.239 , $P = 0.042$) and between the average outer retinal thickness and the axial length (partial
184 correlation analysis adjusted by the average GCC thickness: $r = -0.335$, $P = 0.004$).

185

186 Discussion

187 In the present study, we assessed the relationships between the demographic and clinical variables and
188 the GCC thickness in moderately myopic eyes. We found that GCC thickness is affected by axial
189 length, but that the G/T and G/O ratios are not.

190 SD-OCT is a recent technique that has enabled the imaging of ocular structures with a higher
191 resolution and a faster scan rate than before. Thus, over the past few years, SD-OCT has progressively
192 replaced time-domain OCT for the evaluation of glaucoma. Imaging modalities such as OCT may be
193 effective in these types of cases. The RTVue-100 is an available OCT device that utilizes SD-OCT
194 technology. The RTVue-100 has made it possible to perform automatic measurements of GCC

195 thickness, which is the sum of the nerve fibers, ganglion cells, and IPL [24]. Studies using this
196 instrument have demonstrated that when the early stages of glaucoma were closely monitored, an
197 improved diagnostic ability was associated with these changes [25–31]. However, GCC thickness in
198 healthy eyes has been shown to vary from 76.6 to 119.8 μm [25], in addition to being influenced by
199 axial length, age, and ethnicity [20, 21, 32].

200 Previous OCT studies in myopic patients have focused on the cpRNFL thickness distribution [13–19,
201 33]. Hoh et al. [33] reported no correlation between myopia and cpRNFL thickness. Their study may
202 have been limited by the poorer resolution of the earlier generation OCT (OCT-1). Many other
203 researchers have reported that the average cpRNFL thickness decreased with myopia in conjunction
204 with an increase in the axial length. Using Stratus OCT, Budenz et al. [13] found that the mean
205 cpRNFL thickness was significantly associated with axial length ($P < 0.001$). They found a reduction
206 of 2.2 μm per extra 1 mm of axial length. In other studies of Stratus OCT, Leung et al. [14] and
207 Rauscher et al. [15] found that the mean cpRNFL thickness was significantly associated with axial
208 length ($r = -0.314$, $P = 0.001$ and $r = -0.70$, $P < 0.001$, respectively). A SD-OCT study by Wang et al.
209 [16] that used Cirrus HD-OCT determined that the average cpRNFL thickness decreased as the degree
210 of myopia increased. These findings can be explained by the fact that globe elongation is associated
211 with thinning of the globe wall, which results in a thin cpRNFL [34, 35], or by the axial
212 length-induced magnification effect [19]. In our study, we found that the average cpRNFL thickness
213 decreased with the spherical equivalent and increased with axial length.

214 The thicknesses of the cpRNFL and the GCC significantly decrease with age [20, 32, 36, 37].
215 However, Zhao et al. [21] and our current work showed no correlation between age and GCC
216 thickness.

217 Our study demonstrated a significant negative correlation between GCC thickness and axial length
218 and a significant positive correlation between GCC thickness and the spherical equivalent. We found a
219 reduction of 1.62 μm per extra 1 mm of axial length. The relationship between the GCC and axial
220 length was similar to that found for the cpRNFL thickness and axial length. This can be explained by
221 the fact that globe elongation is associated with thinning of the globe wall, which results in a relatively
222 thin GCC. Very few studies have examined the relationship between GCC thickness and axial length

223 [20, 21]. Kim et al. [20] used the same OCT and investigated the relationship between the GCC
224 thickness and the axial length. Using multiple linear regression analysis, they found that the average
225 and inferior GCC thicknesses were significantly correlated with axial length ($P = 0.021$ and $P = 0.002$;
226 respectively). Zhao et al. [21] showed that the significant reduction in the average GCC thickness was
227 correlated with the axial length ($r = -0.280$, $P = 0.004$). As there are wide variations in the refractive
228 error [38], these variations should be considered when evaluating GCC thickness in myopic eyes.
229 Furthermore, we found a significant correlation between the outer retinal thickness and the axial
230 length ($r = -0.444$, $P < 0.001$), and between the average outer retinal thickness and the average GCC
231 thickness ($r = 0.429$, $P < 0.001$). Our multiple regression analysis also indicated significant
232 correlations between the average GCC thickness and the axial length ($P = 0.03$) and between the
233 average GCC thickness and the outer retinal thickness ($P = 0.02$).

234 GCC thickness has been reported to decrease from the very early stages of glaucoma [24]. Therefore,
235 GCC thickness decreases for both glaucoma and myopic eyes. In the case of glaucoma with myopia, it
236 is difficult to determine whether the decrease in GCC thickness is due to myopia or glaucoma.
237 Although previous studies have shown that the outer retinal thickness, which is measured by OCT, is
238 not affected by glaucoma [9, 24, 30], another study has demonstrated that the outer retinal thickness is
239 affected by myopia [20]. We created two new ratio parameters. In our study, we found the average
240 G/T ratio to be 35.53 %, and the average G/T ratio was not significantly correlated with either the axial
241 length or the spherical equivalent. That is, as the axial length increases, both the GCC and the total
242 retinal thicknesses decrease, so the ratio does not change. The average G/O ratio was 55.43 %, and,
243 similar to the G/T ratio, was not significantly correlated with either the axial length or the spherical
244 equivalent. This indicates that, as the axial length increases, both the GCC and the outer retinal
245 thicknesses decrease, so the ratio does not change. In addition, this latter finding is supported by our
246 results that show a significant correlation between the GCC thickness and the outer retinal thickness
247 (partial correlation analysis adjusted by axial length: $r = 0.312$, $P = 0.007$). Therefore, these findings
248 demonstrate that these new ratio parameters are not affected by myopia.

249 With regard to glaucoma diagnostic ability, the GCC thickness has been shown to be comparable and
250 complementary to the cpRNFL thickness [25, 27–31]. Also, it has been reported that in severely

251 myopic eyes, the diagnostic capability of the GCC thickness is better than that of the cpRNFL
252 thickness [11, 12]. Based on these results, the goal of our study was to investigate whether the ratio
253 parameters might be useful for diagnosing glaucoma. We previously reported finding that the G/T
254 ratio was useful for diagnosing glaucoma with low myopia [22]. Therefore, an investigation of the
255 glaucoma diagnostic capability in moderately and highly myopic eyes needs to be undertaken in the
256 future.

257 Our study has a few limitations. Its relatively small sample size, inclusion of participants of a single
258 ethnicity, and its range of mildly to highly myopic eyes may have resulted in some bias. Further
259 investigation is needed to determine whether the ratio parameters and axial length in highly myopic
260 eyes and in other ethnic groups are correlated. Also, it should be noted that the RTVue-100 cannot
261 correct for magnification effects, so there is a chance that our results may have been different if this
262 correction had been available.

263 In conclusion, the GCC thickness was significantly correlated with both the axial length and the
264 spherical equivalent. Since the SD-OCT measurement of GCC thickness is affected by myopia,
265 evaluation of GCC thickness should be interpreted in the context of axial length. Moreover, the G/T
266 and G/O ratios are suitable parameters for taking into account variations in axial length.

267

268 **Acknowledgments**

269 This study was supported in part by a Grant-in-Aid for Scientific Research (C) 24592656 from the
270 Ministry of Education, Culture, Sports, and Technology of the Japanese Government.

271 **References**

- 272 1. Shimizu N, Nomura H, Ando F, Niino N, Miyake Y, Shimokata H. Refractive errors and factors
273 associated with myopia in an adult Japanese population. *Jpn J Ophthalmol.* 2003;47:6–12.
- 274 2. Mitchell P, Hourihan F, Sandbach J, Wang JJ. The relationship between glaucoma and myopia: the
275 Blue Mountains Eye Study. *Ophthalmology.* 1999;106:2010–5.
- 276 3. Kanamori A, Nakamura M, Escano MF, Seya R, Maeda H, Negi A. Evaluation of the glaucomatous
277 damage on retinal nerve fiber layer thickness measured by optical coherence tomography. *Am J*
278 *Ophthalmol.* 2003;135:513–20.
- 279 4. Wollstein G, Ishikawa H, Wang J, Beaton SA, Schuman JS. Comparison of three optical coherence
280 tomography scanning areas for detection of glaucomatous damage. *Am J Ophthalmol.*
281 2005;139:39–43.
- 282 5. Ojima T, Tanabe T, Hangai M, Yu S, Morishita S, Yoshimura N. Measurement of retinal nerve fiber
283 layer thickness and macular volume for glaucoma detection using optical coherence tomography.
284 *Jpn J Ophthalmol.* 2007;51:197–203.
- 285 6. Wollstein G, Schuman JS, Price LL, Aydin A, Beaton SA, Stark PC, et al. Optical coherence
286 tomography (OCT) macular and peripapillary retinal nerve fiber layer measurements and
287 automated visual fields. *Am J Ophthalmol.* 2004;138:218–25.
- 288 7. Leung CK, Chan WM, Yung WH, Ng AC, Woo J, Tsang MK, et al. Comparison of macular and
289 peripapillary measurements for the detection of glaucoma: an optical coherence tomography study.
290 *Ophthalmology.* 2005;112:391–400.
- 291 8. Medeiros FA, Zangwill LM, Bowd C, Vessani RM, Susanna R Jr, Weinreb RN. Evaluation of retinal
292 nerve fiber layer, optic nerve head, and macular thickness measurements for glaucoma detection
293 using optical coherence tomography. *Am J Ophthalmol.* 2005;139:44–55.
- 294 9. Vajaranant TS, Anderson RJ, Zelkha R, Zhang C, Wilensky JT, Edward DP, et al. The relationship
295 between macular cell layer thickness and visual function in different stages of glaucoma. *Eye.*
296 2011;25:612–8.
- 297 10. Leung CK, Yu M, Weinreb RN, Mak HK, Lai G, Ye C, et al. Retinal nerve fiber layer imaging with
298 spectral-domain optical coherence tomography: interpreting the RNFL maps in healthy myopic

- 299 eyes. *Invest Ophthalmol Vis Sci.* 2012;53:7194–200.
- 300 11. Kim NR, Lee ES, Seong GJ, Kang SY, Kim JH, Hong S, et al. Comparing the ganglion cell
301 complex and retinal nerve fiber layer measurements by Fourier domain OCT to detect glaucoma in
302 high myopia. *Br J Ophthalmol.* 2011;95:1115–21.
- 303 12. Shoji T, Sato H, Ishida M, Takeuchi M, Chihara E. Assessment of glaucomatous changes in
304 subjects with high myopia using spectral domain optical coherence tomography. *Invest Ophthalmol*
305 *Vis Sci.* 2011;52:1098–102.
- 306 13. Budenz DL, Anderson DR, Varma R, Schuman J, Cantor L, Savell J, et al. Determinants of normal
307 retinal nerve fiber layer thickness measured by Stratus OCT. *Ophthalmology.* 2007;114:1046–52.
- 308 14. Leung CK, Mohamed S, Leung KS, Cheung CY, Chan SL, Cheng DK, et al. Retinal nerve fiber
309 layer measurements in myopia: an optical coherence tomography study. *Invest Ophthalmol Vis Sci.*
310 2006;47:5171–6.
- 311 15. Rauscher FM, Sekhon N, Feuer WJ, Budenz DL. Myopia affects retinal nerve fiber layer
312 measurements as determined by optical coherence tomography. *J Glaucoma.* 2009;18:501–5.
- 313 16. Wang G, Qiu KL, Lu XH, Sun LX, Liao XJ, Chen HL, et al. The effect of myopia on retinal nerve
314 fiber layer measurement: a comparative study of spectral-domain optical coherence tomography
315 and scanning laser polarimetry. *Br J Ophthalmol.* 2011;95:255–60.
- 316 17. Kang SH, Hong SW, Im SK, Lee SH, Ahn MD. Effect of myopia on the thickness of the retinal
317 nerve fiber layer measured by Cirrus HD optical coherence tomography. *Invest Ophthalmol Vis Sci.*
318 2010;51:4075–83.
- 319 18. Savini G, Barboni P, Parisi V, Carbonelli M. The influence of axial length on retinal nerve fiber
320 layer thickness and optic-disc size measurements by spectral-domain OCT. *Br J Ophthalmol.*
321 2012;96:57–61.
- 322 19. Öner V, Aykut V, Taş M, Alakus MF, İrsan Y. Effect of refractive status on peripapillary
323 retinal nerve fibre layer thickness: a study by RTVue spectral domain optical coherence
324 tomography. *Br J Ophthalmol.* 2013;97:75–9.
- 325 20. Kim NR, Kim JH, Lee J, Lee ES, Seong GJ, Kim CY. Determinants of perimacular inner retinal
326 layer thickness in normal eyes measured by Fourier-domain optical coherence tomography. *Invest*

- 327 Ophthalmol Vis Sci. 2011;52:3413–8.
- 328 21. Zhao Z, Jiang C. Effect of myopia on ganglion cell complex and peripapillary retinal nerve fibre
329 layer measurements: a Fourierdomain optical coherence tomography study of young Chinese
330 persons. Clin Exp Ophthalmol. 2013;41:561–6. doi:10.1111/ceo. 12045.
- 331 22. Kita Y, Kita R, Takeyama A, Takagi S, Nishimura C, Tomita G. Ability of optical coherence
332 tomography-determined ganglion cell complex thickness to total retinal thickness ratio to diagnose
333 glaucoma. J Glaucoma. 2012;. doi:10.1097/IJG. 0b013e31825af58a.
- 334 23. Kita Y, Kita R, Takeyama A, Anraku A, Tomita G, Goldberg I. Relationship between macular
335 ganglion cell complex thickness and macular outer retinal thickness: a spectral-domain optical
336 coherence tomography study. Clin Exp Ophthalmol. 2013;41:674–82. doi:10.1111/ceo.12089.
- 337 24. Tan O, Li G, Lu AT, Varma R, Huang D. Mapping of macular substructures with optical coherence
338 tomography for glaucoma diagnosis. Ophthalmology. 2008;115:949–56.
- 339 25. Tan O, Chopra V, Lu AT, Schuman JS, Ishikawa H, Varma R, et al. Detection of macular ganglion
340 cell loss in glaucoma by Fourier-domain optical coherence tomography. Ophthalmology.
341 2009;116:2305–14.
- 342 26. Kita Y, Kita R, Nitta A, Nishimura C, Tomita G. Glaucomatous eye macular ganglion cell complex
343 thickness and its relation to temporal circumpapillary retinal nerve fiber layer thickness. Jpn J
344 Ophthalmol. 2011;55:228–34.
- 345 27. Kim NR, Lee ES, Seong GJ, Kim JH, An HG, Kim CY. Structure–function relationship and
346 diagnostic value of macular ganglion cell complex measurement using Fourier-domain OCT in
347 glaucoma. Invest Ophthalmol Vis Sci. 2010;51:4646–51.
- 348 28. Rao HL, Zangwill LM, Weinreb RN, Sample PA, Alencar LM, Medeiros FA. Comparison of
349 different spectral domain optical coherence tomography scanning areas for glaucoma diagnosis.
350 Ophthalmology. 2010;117:1692–9.
- 351 29. Seong M, Sung KR, Choi EH, Kang SY, Cho JW, Um TW, et al. Macular and peripapillary retinal
352 nerve fiber layer measurements by spectral domain optical coherence tomography in normaltension
353 glaucoma. Invest Ophthalmol Vis Sci. 2010;51:1446–52.
- 354 30. Schulze A, Lamparter J, Pfeiffer N, Berisha F, Schmidtman I, Hoffmann EM. Diagnostic ability

- 355 of retinal ganglion cell complex, retinal nerve fiber layer, and optic nerve head measurements by
356 Fourier-domain optical coherence tomography. *Graefes Arch Clin Exp Ophthalmol.*
357 2011;249:1039–45.
- 358 31. Mori S, Hangai M, Sakamoto A, Yoshimura N. Spectral-domain optical coherence tomography
359 measurement of macular volume for diagnosing glaucoma. *J Glaucoma.* 2010;19:528–34.
- 360 32. Girkin CA, McGwin G Jr, Sinai MJ, Sekhar GC, Fingeret M, Wollstein G, et al. Variation in optic
361 nerve and macular structure with age and race with spectral-domain optical coherence tomography.
362 *Ophthalmology.* 2011;118:2403–8.
- 363 33. Hoh ST, Lim MC, Seah SK, Lim AT, Chew SJ, Foster PJ, et al. Peripapillary retinal nerve fiber
364 layer thickness variations with myopia. *Ophthalmology.* 2006;113:773–7.
- 365 34. Apple DJ, Fabb MF. Clinico-pathologic correlation of ocular disease: a text and stereoscopic atlas.
366 St. Louis: CV Mosby; 1978. p. 39–44.
- 367 35. Yanoff M, Fine BS. Ocular pathology: a text and atlas. Philadelphia: Harper & Row; 1982. p.
368 513–4.
- 369 36. Kanamori A, Escano MF, Eno A, Nakamura M, Maeda H, Seya R, et al. Evaluation of the effect of
370 aging on retinal nerve fiber layer thickness measured by optical coherence tomography.
371 *Ophthalmologica.* 2003;217:273–8.
- 372 37. Hirasawa H, Tomidokoro A, Araie M, Konno S, Saito H, Iwase A, et al. Peripapillary retinal nerve
373 fiber layer thickness determined by spectral-domain optical coherence tomography in
374 ophthalmologically normal eyes. *Arch Ophthalmol.* 2010;128:1420–6.
- 375 38. Iwase A, Tomidokoro A, Araie M, Shirato S, Shimizu H, Kitazawa Y, Tajimi Study Group.
376 Performance of frequency-doubling technology perimetry in a population-based prevalence survey
377 of glaucoma: the Tajimi study. *Ophthalmology.* 2007;114:27–32.

378

379

380 **Figure legends**

381 **Fig. 1**

382 A typical example of a vertical OCT scan. The image segmentation algorithm automatically detected
383 the retinal layer boundaries (white lines) and measured the ganglion cell complex thickness (a), outer
384 retinal thickness (b), and total retinal thickness (c). These retinal layers are marked by arrows

385 **Fig. 2**

386 Relationships between the macular parameters and the axial length. The GCC thickness is significantly
387 associated with axial length ($r = -0.384$, $P = 0.001$): the regression formula is $y = -1.62x + 133.74$. The
388 outer retinal thickness is significantly associated with axial length ($r = -0.444$, $P < 0.001$): the
389 regression formula is $y = -2.32x + 226.07$. No significant association was observed between the G/T
390 ratio and the axial length ($r = -0.093$, $P = 0.428$)

Table 1 Characteristics of the study participants (n = 74)

Variable	Mean \pm SD	95% CI
Sex		
Male	47	
Female	27	
Age (years)	34.88 \pm 7.02	33.25 to 36.50
IOP (mmHg)	14.15 \pm 2.53	13.56 to 14.73
Spherical equivalent (D)	-3.47 \pm 2.96	-4.15 to -2.78
Axial length (mm)	25.05 \pm 1.38	24.73 to 25.37
MD (dB)	-0.66 \pm 1.11	-0.92 to -0.40
PSD (dB)	1.40 \pm 0.50	1.28 to 1.51

CI confidence interval, *IOP* intraocular pressure, *D* diopter, *MD* mean deviation, *PSD* pattern standard deviation

Table 2 Optical coherence tomography parameter measurements obtained using the RTVue-100

	Study participants (n = 74)	95% CI
	Mean \pm SD	
GCC thickness (μm)		
Average thickness	93.07 \pm 5.84	91.72 - 94.42
Superior thickness	93.28 \pm 6.12	91.86 - 94.70
Inferior thickness	92.86 \pm 6.13	91.44 - 94.28
<i>G/T</i> ratio (%)		
Average	35.64 \pm 1.34	35.32 - 35.95
Superior	35.39 \pm 1.40	35.07 - 35.71
Inferior	35.90 \pm 1.47	35.56 - 36.24
<i>G/O</i> ratio (%)		
Average	55.43 \pm 3.30	54.67 - 56.20
Superior	54.85 \pm 3.41	54.06 - 55.64
Inferior	56.09 \pm 3.61	55.25 - 56.92
Outer retinal thickness (μm)		
Average thickness	168.00 \pm 7.21	166.33 - 169.67
Superior thickness	170.20 \pm 7.49	168.46 - 171.93
Inferior thickness	165.69 \pm 7.29	164.00 - 167.38
Total retinal thickness (μm)		

Average thickness	261.07 ± 11.05	258.51 - 263.63
Superior thickness	263.48 ± 11.51	260.81 - 266.15
Inferior thickness	258.55 ± 11.18	255.96 - 261.14
cpRNFL thickness (µm)		
Average thickness	102.67 ± 8.70	100.65 - 104.68
Superior thickness	103.23 ± 10.67	100.76 - 105.70
Inferior thickness	103.05 ± 13.06	100.02 - 106.08
Temporal quadrant	84.41 ± 13.34	81.32 - 87.50
Superior quadrant	125.68 ± 15.62	122.07 - 129.30
Nasal quadrant	68.25 ± 9.24	66.11 - 70.39
Inferior quadrant	131.03 ± 15.79	127.37 - 134.68

CI confidence interval, *GCC* macular ganglion cell complex, *G/T ratio* ganglion cell complex thickness to total retinal thickness ratio, *G/O ratio* ganglion cell complex thickness to outer retinal thickness ratio, *cpRNFL* circumpapillary retinal nerve fiber layer

Table 3 Correlations between OCT parameters and axial length, spherical equivalent, age, and outer retinal thickness

	Axial length		Spherical equivalent		Age		Outer retinal thickness	
	<i>r</i>	<i>P</i>	<i>r</i>	<i>P</i>	<i>r</i>	<i>P</i>	<i>r</i>	<i>P</i>
GCC thickness								
Average thickness	-0.384	0.001*	0.436	< 0.001*	0.028	0.810	0.429	< 0.001*
Superior thickness	-0.346	0.002*	0.381	0.001*	-0.003	0.979	0.390	0.001*
Inferior thickness	-0.386	0.001*	0.450	< 0.001*	0.056	0.633	0.429	< 0.001*
Outer retinal thickness								
Average thickness	-0.444	< 0.001*	0.406	< 0.001*	0.024	0.842	NA	NA
Superior thickness	-0.477	< 0.001*	0.440	< 0.001*	-0.016	0.889	NA	NA
Inferior thickness	-0.402	< 0.001*	0.360	0.002*	0.071	0.547	NA	NA
Total retinal thickness								
Average thickness	-0.493	< 0.001*	0.495	< 0.001*	0.030	0.797	0.879	< 0.001*
Superior thickness	-0.495	< 0.001*	0.489	< 0.001*	-0.012	0.917	0.845	< 0.001*
Inferior thickness	-0.474	< 0.001*	0.482	< 0.001*	0.077	0.513	0.871	< 0.001*
cpRNFL thickness								
Average thickness	-0.512	< 0.001*	0.514	< 0.001*	0.029	0.804	0.337	0.003*
Superior thickness	-0.485	< 0.001*	0.503	< 0.001*	0.009	0.936	0.285	0.014*
Inferior thickness	-0.264	0.023*	0.187	0.110	0.138	0.243	0.322	0.005*
Temporal quadrant	0.018	0.882	-0.165	0.160	-0.165	0.160	0.004	0.971
Superior quadrant	-0.466	< 0.001*	0.491	< 0.001*	0.048	0.685	0.335	0.004*

Nasal quadrant	-0.448	< 0.001*	0.660	< 0.001*	0.188	0.110	0.254	0.029*
Inferior quadrant	-0.453	< 0.001*	0.506	< 0.001*	-0.082	0.489	0.139	0.236

r: Pearson correlation coefficient, *GCC* macular ganglion cell complex, *cpRNFL* circumpapillary retinal nerve fiber layer

**P* < 0.05

Table 4. Correlations between ratio parameters and axial length, spherical equivalent, and age

	Axial length		Spherical equivalent		Age	
	<i>r</i>	<i>P</i>	<i>r</i>	<i>P</i>	<i>r</i>	<i>P</i>
<i>G/T</i> ratio						
Average	-0.093	0.428	0.173	0.140	0.013	0.914
Superior	-0.031	0.793	0.092	0.436	0.008	0.947
Inferior	-0.133	0.257	0.224	0.055	0.010	0.930
<i>G/O</i> ratio						
Average	-0.091	0.440	0.172	0.144	0.014	0.904
Superior	-0.033	0.783	0.095	0.419	0.007	0.953
Inferior	-0.127	0.281	0.219	0.061	0.013	0.909

r: Pearson correlation coefficient

G/T ratio ganglion cell complex thickness to total retinal thickness ratio, *G/O ratio* ganglion cell complex thickness to outer retinal thickness ratio

Table 5 Results of the multiple linear regression analysis of the relationships between ganglion cell complex thickness (dependent variable) and age, sex, axial length, and macular outer retinal thickness

Independent variable	Partial regression coefficient	95% CI		Standardized partial regression coefficient	<i>P</i> value
Age (years)	-0.03	-0.23	0.18	-0.04	0.77
Sex	-1.15	-4.20	1.90	-0.10	0.45
Axial length (mm)	-1.11	-2.14	-0.09	-0.26	0.03
Outer retinal thickness (μm)	0.24	0.05	0.44	0.30	0.02

CI confidence interval

Figure 1.

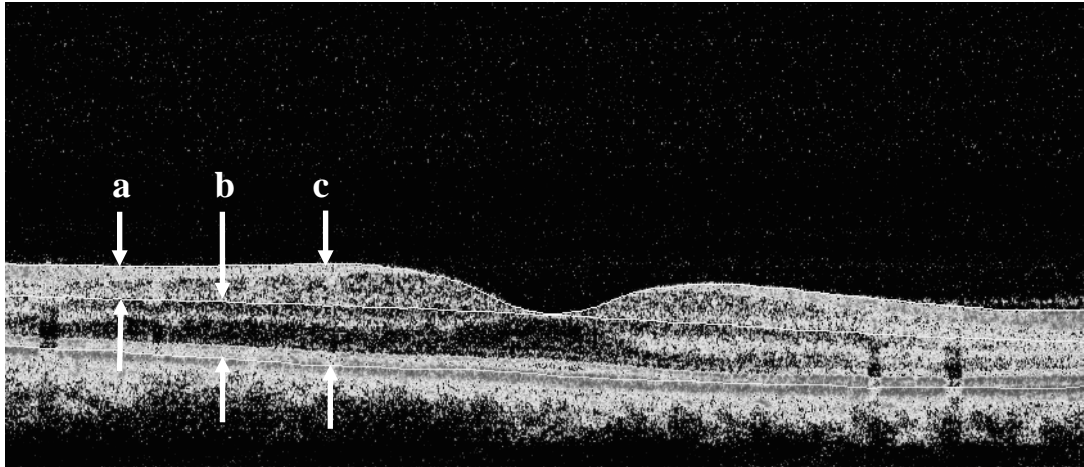


Figure 2.

